Attempt to Generate Strong Basicity on Silica and Titania

ARTICLE *in* THE JOURNAL OF PHYSICAL CHEMISTRY C · MARCH 2008

Impact Factor: 4.77 · DOI: 10.1021/jp710213j

6 AUTHORS, INCLUDING:

Lin-Bing Sun
Nanjing Tech University
72 PUBLICATIONS **1,535** CITATIONS
SEE PROFILE

Ying Wang
Wright State University
270 PUBLICATIONS **2,671** CITATIONS
SEE PROFILE

Attempt to Generate Strong Basicity on Silica and Titania

Lin Bing Sun,[†] Fang Na Gu,[†] Yuan Chun,[†] Jing Yang,[†] Ying Wang,[‡] and Jian Hua Zhu*[,†]

Key Laboratory of Mesoscopic Chemistry of MOE, School of Chemistry and Chemical Engineering, and Ecomaterials and Renewable Energy Research Center, Nanjing University, Nanjing 210093, China

Received: October 22, 2007; In Final Form: January 14, 2008

Modification and control of surface function on porous materials have been a very promising and appealing area of chemistry. In this paper, the reason as to why it is impossible to generate a strong basicity on silica and titania is explored in detail, and consequently, a new strategy was adopted to overcome this obstacle, not only to obtain a solid strong base derived from silica and titania for the first time but also in a new environmentally benign way. Base precursor KNO_3 was loaded on silica and titania along with alumina and zirconia for comparison. Varied dispersion and thermal decomposition behavior of KNO_3 on these supports as well as the different resulting basicity of the composites were delineated, and the surface vacant sites and electronegativity of cations in supports were proven to be responsible for such differences. Further, a redox strategy was employed to convert the supported KNO_3 to basic sites at relatively mild conditions, through which a strong basicity was finally generated on silica and titania, while superbasicity was formed on alumina and zirconia. Moreover, the present redox strategy could significantly reduce the release of harmful gases such as nitrogen oxides, which is beneficial to the protection of the environment. The different mechanisms for the thermal activation and redox approach on the preparation of solid strong basic materials were determined.

Introduction

Design and preparation of new functional materials are crucial to the chemical industry, especially for the development of adsorption and catalysis. Among these efforts, the research concerning solid strong bases is meaningful for developing environmentally benign and economical catalytic processes because they can catalyze diverse reactions under mild conditions and reduce the production of pollutants. Aimed at industrial applications, these new catalysts or adsorbents should be based on inexpensive or easily available materials. However, amorphous silica is an exception to the investigation of solid strong bases.

Siliceous materials have been used extensively in catalysis, adsorption, and separation because of their low cost, high surface area, and abundant porosity. By use of surfactant supramolecular templates, an incredible degree of control can be achieved on silica with various pore symmetries, such as hexagonal,[1] cubic,[2] lamellar,[3] and wormhole.[4] Silica-based materials have been processed into a diversity of morphologies including spheres,[5] helicoids,[6] fibers,[7] and thin films.[8] Moreover, a large number of structures found in nature presenting complex architectures (the case of diatoms or radiolaria) are silica-based.[9] Consequently, silica could be an ideal starting material to prepare solid bases with a high surface area, tunable pore size, and diverse morphology. Unfortunately, generating a strong basicity on silica is so difficult that less attention is paid to the solid bases derived from silica in comparison to those from alumina or zirconia.[10−14] For instance, loading KNO_3 on alumina or zirconia could create superbasicity[13,14] but only form weakly basic sites on silica or titania.[15] To date, it is not fully understood as to what causes such a significantly different basicity on the oxides supported by KNO_3. It is a challenge to establish strongly basic sites on silica or titania, which is not only meaningful for the study of material chemistry but also particularly valuable for potential industrial applications because silica and titania have been widely used in industry.[16,17]

Many attempts have been made to form a strong basicity on porous oxides through the incorporation of basic guests.[18−20] Doping sodium hydroxide and metal sodium[10] or impregnating an ammoniacal solution of potassium[11] on alumina can produce solid superbases. The hydroxides of alkali metals supported on alumina can also exhibit a strong basicity if activated properly.[12] However, most of these solid bases are oxygen-sensitive and/or easily poisoned with atmospheric CO_2, making preparation and storage difficult.[14] To overcome these drawbacks, neutral salts KNO_3 and KF were introduced as base precursors.[21−27] Since the basicity of these neutral salt-containing composites is only generated in the activation prior to reaction, the contamination with atmospheric CO_2 can be avoided so that they are highly efficient in catalytic processes.[13,14,25−27] In general, a specific host material is required for supporting the neutral guest, namely, it should provide a suitable surface to disperse the neutral salt; moreover, the surface should have a suitable interaction with the salt to form basic sites in the process of thermal activation.[13] However, only a few materials (e.g., alumina) can meet such rigorous demands to act as an eligible support for neutral guests. Hence, it is necessary to seek a new strategy to form a strong basicity on those common supports (e.g., silica) modified with the neutral guest. Additionally, another two factors may hinder the applications of the KNO_3-derived solid bases. One is the high temperature ($\geq$600 °C) needed for the thermal decomposition of KNO_3;[28] the other is the release of harmful gases such as nitrogen oxides (NO_x) during KNO_3 decomposition.[29,30] Therefore, it is desirable to develop an environmentally benign approach to convert supported KNO_3 at relatively low temperatures.

* Corresponding author. E-mail: jhzhu@nju.edu.cn; fax: +86-25-83317761; tel: +86-25-83595848.
[†] School of Chemistry and Chemical Engineering.
[‡] Ecomaterials and Renewable Energy Research Center.

10.1021/jp710213j CCC: $40.75
Published on Web 03/04/2008

TABLE 1: Physical Properties of Different Supports

support	S_{BET} ($m^2\ g^{-1}$)	V_{total}[a] ($cm^3\ g^{-1}$)	V_{micro}[b] ($cm^3\ g^{-1}$)	D_p[c] (nm)	dispersion capacity ($K^+\ nm^{-2}$) calcd[d]	dispersion capacity ($K^+\ nm^{-2}$) measured[e]	electronegativity of cation (χ_i)
Al_2O_3	208	0.393	0.002	6.2	4.4	4.5	11.27
ZrO_2	120	0.207	0	6.2	8.6	8.4	11.97
TiO_2[f]	52	0.099	0	13.8	7.0	6.9	13.86
SiO_2	411	0.942	0.020	7.2	0	0.1	17.10

[a] Total pore volume. [b] Micropore volume. [c] BJH desorption average pore diameter. [d] Calculated according to surface vacant site density. [e] Measured by XRD quantitative analysis. [f] Anatase.

The first aim of this study was to explore as to what hinders the generation of a strong basicity on silica and titania; for comparison, alumina and zirconia are employed. The base precursor KNO_3 was loaded on these oxide supports to investigate the dispersion and thermal decomposition behavior of the guest. The relationship between the structural properties of the host and the basicity generated on the composite was examined. The second aim was to generate a strong basicity on silica and titania through a new redox strategy. The supported neutral salt KNO_3 was converted to a basic species with the assistance of a controllable chemical reaction at mild conditions. The redox strategy also could greatly suppress the release of NO_x.

Experimental Procedures

Materials. KNO_3 (AR grade) and titania were provided by Shanghai Chemical. Alumina (γ-type), zirconia, and silica were the products of Nanjing Inorganic Chemical, Toray Ltd., and Qingdao Haiyang Chemical, respectively. Their surface areas are listed in Table 1. Methanol, ethanol, 2-propanol, and *t*-butanol are commercially available reagents (AR grade).

Preparation. KNO_3 was loaded on alumina, zirconia, titania, and silica by wet impregnation. In a typical synthesis, a given amount of KNO_3 was dissolved in 10 mL of water, and then 1.0 g of the support was added. After stirring at room temperature for 24 h, the mixture was evaporated at 80 °C followed by drying at 100 °C overnight. Since the surface areas of supports are different, the amount of KNO_3 loaded is expressed in terms of a surface K^+ density (i.e., the number of K^+ ions per unit surface area of the supports). The name of catalysts is denoted as, for example, $10KNO_3/SiO_2$, which means 10 $K^+\ nm^{-2}$ of KNO_3 was supported on silica.

Characterization. XRD patterns of samples were recorded with a Rigaku D/max-rA system using Cu Kα radiation in the 2θ range from 5 to 70° at 40 kV and 40 mA. FTIR measurements were performed on a Bruker 22 FTIR spectrometer by means of the KBr pellet technique. Each wafer consisted of 2 mg of sample and 18 mg of KBr with a diameter of 13 mm. The spectra were collected with a 2 cm^{-1} resolution. The N_2 adsorption−desorption isotherms were measured using a Micromeritics ASAP 2020 system at −196 °C, for which the sample was outgassed at 300 °C for 4 h prior to analysis. The BET specific surface area was calculated using desorption data in a relative pressure (p/p_0) ranging from 0.04 to 0.20.

TG-MS analysis of the sample was conducted on a thermobalance (STA-499C, NETZSCH) coupled to a mass analyzer (QUADSTAR-422, PFEIFFER). Methanol was introduced into the system by bubbling the methanol saturation vapor generator at 25 °C with an Ar flow of 20 mL min^{-1}. The sample was kept at 25 °C for 1 h to obtain a stable state and then heated from 25 to 800 °C at 8 °C min^{-1} in a continuous flow of Ar. The ionization of the decomposition products was performed with an ion source of electron impact at 70 eV. Temperature programmed decomposition (TPDE) of KNO_3 supported on oxides was carried out in a flow reactor. The sample was heated from 25 to 450 °C at a rate of 8 °C min^{-1} and kept at 450 °C for a given time. Methanol was introduced with a syringe pump at a rate of 1.2 mL $g^{-1}\ h^{-1}$, in which N_2 (20 mL min^{-1}) was used as a carrier gas. The NO_x liberated in the process was converted to NO_2 through a CrO_3 tube and subsequently detected by the colorimetric method, representing the amount of KNO_3 decomposed.[14] The reduction of NO_x was determined from the amount measured in the TPDE process and the amount calculated theoretically.

The base strength of the sample was detected by a series of Hammett indicators.[14] The indicators included bromothymol blue ($H_- = 7.2$), phenolphthalein ($H_- = 9.3$), 2,4-dinitroaniline ($H_- = 15.0$), 4-nitroaniline ($H_- = 18.4$), benzidine ($H_- = 22.5$), 4-chloroaniline ($H_- = 26.5$), and aniline ($H_- = 27.0$). After being pretreated at the given conditions and cooled to room temperature, the sample was transferred to purified cyclohexane under the protection of N_2. Two drops of indicator solution (0.1 wt % indicator dissolved in benzene) were added to the suspension, and the color change of the indicator on the solid surface was monitored visually. To measure the amount of basic sites, 100 mg of sample was shaken in 10 mL of aqueous HCl (0.05 mol L^{-1}) for 24 h, and the slurry was separated by a centrifuge. The remaining acid in the liquid phase was titrated with aqueous NaOH (0.01 mol L^{-1}), and phenolphthalein was employed as an indicator. To check the dissolution of K^+ in the measurement of the basic site amount, the solution before titration was analyzed by J-A1100 inductively coupled plasma-optical emission spectrometry (ICP-OES).

The KNO_3-modified samples (100 mg) were treated with a reducing agent in a conventional flow reactor at atmospheric pressure, in which the reducing agent was introduced with a syringe pump at a rate of 1.2 mL $g^{-1}\ h^{-1}$, and N_2 (20 mL min^{-1}) was used as a carrier gas. The effects of the methanol amount (0−1.8 mL g^{-1}), KNO_3 loading (0−12 $K^+\ nm^{-2}$), treatment temperature (300−600 °C), and reducing agent type (methanol, ethanol, 2-propanol, and *t*-butanol) were investigated.

Catalytic Test. The catalytic decomposition of 2-propanol was carried out in a conventional flow reactor at atmospheric pressure. A catalyst (50 mg, 20−40 mesh) was treated with methanol (1.2 mL g^{-1}) at 450 °C to generate basic active sites prior to reaction. The reaction was conducted at 450 °C, and N_2 (20 mL min^{-1}) was employed as a carrier gas. The reactant 2-propanol was introduced using a syringe pump with a space velocity of 1.9 h^{-1}. The reaction mixture was analyzed by on-line GC (Varian 3700) equipped with Porapak T column (4 m × 3 mm i.d.).

Results

Dispersion and Thermal Decomposition of Supported KNO_3. Figure 1A shows the nitrogen adsorption−desorption isotherms of Al_2O_3, ZrO_2, TiO_2, and SiO_2. These isotherms have different shapes but possess a hysteresis loop, which can be tentatively ascribed to the mesoporosity and the capillary

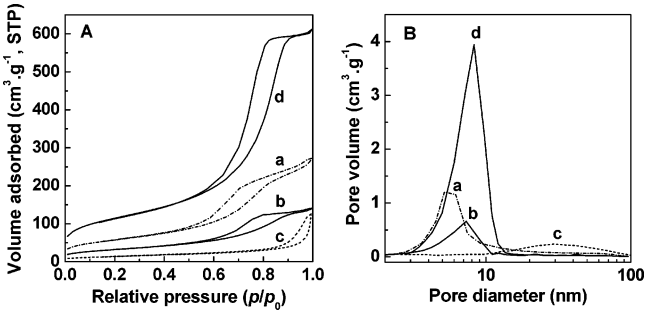

Figure 1. (A) Nitrogen adsorption−desorption isotherms and (B) pore size distributions of (a) Al_2O_3, (b) ZrO_2, (c) TiO_2, and (d) SiO_2.

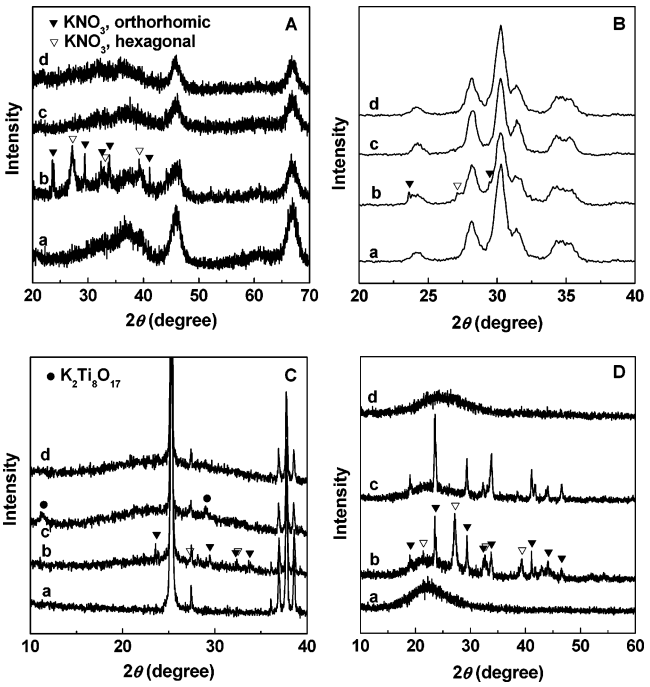

Figure 2. XRD patterns of KNO_3 supported on (A) Al_2O_3, (B) ZrO_2, (C) TiO_2, and (D) SiO_2 with a surface cation density of 10 K^+ nm^{-2}, where a denotes the supports, and b−d denote the KNO_3-modified samples as-prepared, activated at 600 °C, and treated with methanol (1.2 mL g^{-1}) at 450 °C, respectively.

condensation at high pressure.[31] Additionally, the space between oxide particles also is a possible origin of the hysteresis loop. For TiO_2, the inflection point value of relative pressure (p/p_0 > 0.8) is higher than that of other supports ($p/p_0 = \sim 0.5$), implying the existence of pores with larger sizes. This inference is confirmed by the pore size distribution in Figure 1B. As seen in Table 1, the BET surface area and pore volume decrease in the order SiO_2 > Al_2O_3 > ZrO_2 > TiO_2. An average pore diameter of 13.8 nm is detected for TiO_2, which is much larger than that of other supports (6.2−7.2 nm).

Figure 2 displays the XRD patterns of Al_2O_3, ZrO_2, TiO_2, and SiO_2 before and after KNO_3 modification. Two different crystalline phases (i.e., orthorhombic (JCPDS card no. 74-2055) and hexagonal (JCPDS card no. 76-1693) phases (curves b, Figure 2)[23]) exist in KNO_3 supported on all oxides. Since the unsupported KNO_3 only possesses the crystalline form of the orthorhombic phase, the hexagonal phase of KNO_3 seems to be formed in the process of sample preparation. Besides, no diffraction line of the hexagonal phase is observed on pure KNO_3 after it is treated with the same process (spectra not shown). This phenomenon indicates the crucial role played by the interaction between KNO_3 and supports in the formation of the hexagonal phase. The diffraction lines of the hexagonal

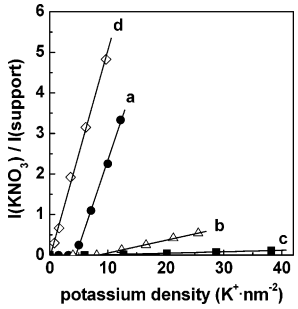

Figure 3. Dispersion of KNO_3 on (a) Al_2O_3, (b) ZrO_2, (c) TiO_2, and (d) SiO_2. The intensity of KNO_3 was calculated from the sum of the line at 23.5 and 27.2° for the orthorhombic and hexaganol phases, respectively, while the intensity of the support was denoted as the line at 66.8, 30.2, 25.3, and 22.0° for Al_2O_3, ZrO_2, TiO_2, and SiO_2, respectively.

phase on Al_2O_3 and SiO_2 obviously are wider than those of the orthorhombic phase, indicating smaller or more amorphous KNO_3 particles in the new phase.

Figure 3 depicts the dispersion of KNO_3 on different supports by XRD quantitative analysis. KNO_3 is difficult to disperse on SiO_2, and the straight line (curve d in Figure 3) almost goes through the origin, corresponding to a low dispersion capacity of 0.1 K^+ nm^{-2} (Table 1). Contrarily, other supports more easily disperse KNO_3, and curves a−c in Figure 3 give an intercept. Consequently, the detected dispersion capacities of KNO_3 on Al_2O_3, ZrO_2, and TiO_2 are 4.5, 8.4, and 6.9 K^+ nm^{-2}, respectively (Table 1). Once the loading amount of KNO_3 exceeds the dispersion capacity, crystalline KNO_3 appears in the XRD patterns of the composites.

As presented in Figure 2, KNO_3-modified samples exhibit different change trends in their XRD patterns after thermal activation at 600 °C. The XRD patterns of KNO_3/Al_2O_3 and KNO_3/ZrO_2 are identical to the support (curves a and c in Figure 2A,B), and the high base strength ($H\_$) of 27.0 emerged on the composites (Table 2). Clearly, the supported KNO_3 decomposed to form strong basic species (Table 2).[13,14] Thermal activation removed KNO_3 diffraction lines from KNO_3/TiO_2; meanwhile, a new phase attributed to $K_2Ti_8O_{17}$ (JCPDS card no. 84-2057)[15] emerged (curve c, Figure 2C), accompanied by a low base strength ($H\_$) of 9.3 (Table 2). Nonetheless, thermal activation of KNO_3/SiO_2 caused an increase in the orthorhombic phase, but the hexagonal phase disappeared (curve c, Figure 2D), which demonstrates the instability of the hexagonal phase of KNO_3 at high temperatures. Since most of the supported KNO_3 is only converted from one crystalline phase to another rather than decomposing to basic species, the base strength ($H\_$) measured on KNO_3/SiO_2 after activation at 600 °C was 9.3 (Table 2). In other words, the same thermal activation resulted in quite a different basicity on four oxides modified by the same neutral salt.

Conversion of Supported KNO_3 by Redox Approach. The diffraction lines of KNO_3 loaded on silica disappeared once the sample of $10KNO_3/SiO_2$ had contact with methanol at 450 °C (curve d, Figure 2D), indicating the conversion of KNO_3 at a relatively low temperature. Figure 4A depicts the IR spectra of $10KNO_3/SiO_2$ recorded at different pretreatment conditions. The bands at 1767, 1385, and 828 cm^{-1} assigned to the vibration of nitrate[32] were detected on the as-prepared sample (curve a, Figure 4A), and no apparent decrease was observed after the sample was thermally activated at 600 °C (curve b, Figure 4A). However, the treatment of methanol at 450 °C causes these bands to decrease, and an evident decline is observed when 0.3 mL g^{-1} methanol is introduced (curve d, Figure 4A). As the

TABLE 2: Base Strength, NO_x Suppression, and 2-Propanol Decomposition of Different Samples

					decomposition of 2-propanol[a]			
	base strength[b] (H_-)				formation rate (S)		formation rate (K)	
sample[c]	A	B	C	suppression of NO_x (%)	propene	acetone	propene	acetone
KNO_3/Al_2O_3	27.0	15.0	27.0	89.1	31.4	0	2.5	24.3
KNO_3/ZrO_2	27.0	15.0	27.0	88.6	30.7	0.5	2.3	15.6
KNO_3/TiO_2	9.3	7.2	22.5	85.9	29.3	1.2	3.0	6.0
KNO_3/SiO_2	9.3	7.2	22.5	90.2	30.4	1.0	6.3	3.2

[a] S: supports and K: KNO_3-modified samples and treated with methanol (1.2 mL g^{-1}) at 450 °C. The unit of formation rate is mmol g^{-1} h^{-1}. [b] A: activated at 600 °C; B: activated at 450 °C; and C: treated with methanol (1.2 mL g^{-1}) at 450 °C. [c] Surface cation density of KNO_3-modified samples was 10 K^+ nm^{-2}.

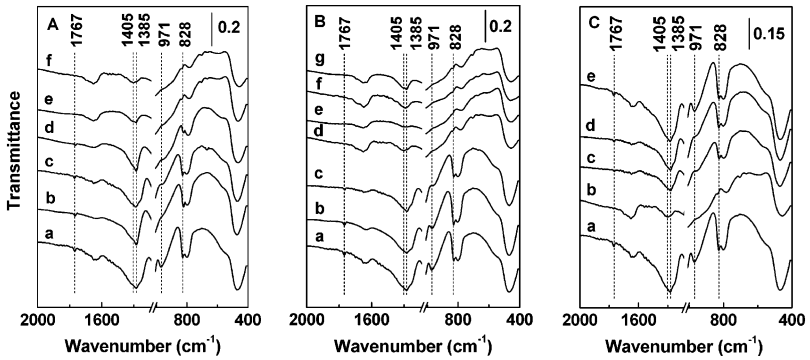

Figure 4. (A) IR spectra of $10KNO_3/SiO_2$ (a) as-prepared, (b) thermally activated at 600 °C, and treated with (c) 0.1, (d) 0.3, (e) 0.6, and (f) 1.2 mL g^{-1} methanol at 450 °C. (B) IR spectra of $10KNO_3/SiO_2$ (a) as-prepared and treated with 1.2 mL g^{-1} methanol at (b) 300, (c) 400, (d) 450, (e) 500, (f) 550, and (g) 600 °C. (C) IR spectra of $10KNO_3/SiO_2$ (a) as-prepared and treated with 1.2 mL g^{-1} (b) methanol, (c) ethanol, (d) 2-propanol, and (e) *t*-butanol at 450 °C.

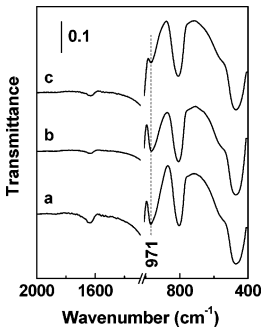

Figure 5. IR spectra of pure SiO_2 (a) unactivated and activated at (b) 450 and (c) 600 °C.

amount of methanol increases, the bands of nitrate become even weaker, whereas the 1405 cm^{-1} band of CO_2 adsorbed on basic sites becomes visible at high methanol dosages.[33] These results confirm the conversion of KNO_3 supported on SiO_2 by methanol treatment at low temperatures, in good agreement with the XRD measurements.

IR analysis also monitors the variation of silanol groups in KNO_3/SiO_2. The 971 cm^{-1} band ascribed to the silanol groups (Si−OH) bending vibration appears on the as-prepared sample (curve a, Figure 4A),[34,35] and its intensity begins to decline when only 0.1 mL g^{-1} methanol is introduced at 450 °C (curve c, Figure 4A). As the dosage of methanol rises, the band of the silanol groups progressively decreases and finally disappears on the $10KNO_3/SiO_2$ sample. Likewise, thermal activation at 600 °C lowers the intensity of the 971 cm^{-1} band on KNO_3/SiO_2 as well (curve b, Figure 4A). To examine the impact of thermal treatment on the consumption of silanol groups, Figure 5 presents the IR spectra of silica pretreated at different temperatures. The intensity of the 971 cm^{-1} band is constant for the samples before and after activation at 450 °C (curves a and b, Figure 5) but much weaker once the sample was activated at 600 °C (curve c, Figure 5), in agreement with the report that the silanol groups on silica can be consumed by calcination at 550 °C.[34] Therefore, for the KNO_3/SiO_2 sample treated with methanol at 450 °C, the consumption of silanol groups originates from the interaction between potassium species and silica surface, whereas for the sample activated at 600 °C, such consumption should be attributed to the thermal effect.

Figure 6A shows the influence of the methanol amount on the basic properties of the KNO_3/SiO_2 samples. A base strength (H_-) of 7.2 was measured for the untreated sample, and it rose to 15.0 once the sample had contact with 0.1 mL g^{-1} methanol. Some strong basic sites ($H_- = 22.5$) emerged when the sample was treated with methanol beyond 0.6 mL g^{-1}. This is the first time that such a high base strength was obtained on SiO_2 supported KNO_3 because the potassium species preferably react with SiO_2 to form a compound with a low base strength if the composite was treated at high temperatures.[36] The amount of basic sites enhances gradually as the methanol dosage rises to 1.2 mL g^{-1}. To check the dissolution of K^+ in the measurement of the basic site amount, the solution used for titration was analyzed by ICP. The result shows that the dissolved potassium species was 3.48 mmol g^{-1} for the $10KNO_3/SiO_2$ sample, which is consistent with the result of the basic site amount (3.39 mmol g^{-1}). This indicates that the potassium species was dissolved in the solution after it reacted with aqueous HCl. Figure 6B delineates the effect of KNO_3 loading on the basicity of the composites. The base strength on the KNO_3/SiO_2 samples rises to $H_- = 22.5$ as the loading amount of KNO_3 achieves a value of 7.8 K^+ nm^{-2}, but the further addition of KNO_3 had no improvement on the base strength of the composite.

Figure 6C demonstrates the impact of treatment temperature on the basicity generated on KNO_3/SiO_2. When the composite contacts with methanol at 300 °C, only a few basic sites (0.11 mmol g^{-1}) with a weak base strength ($H_- = 7.2$) were produced. Increasing the temperature to 450 °C obviously enhanced the number and strength of basic sites on KNO_3/SiO_2. However,

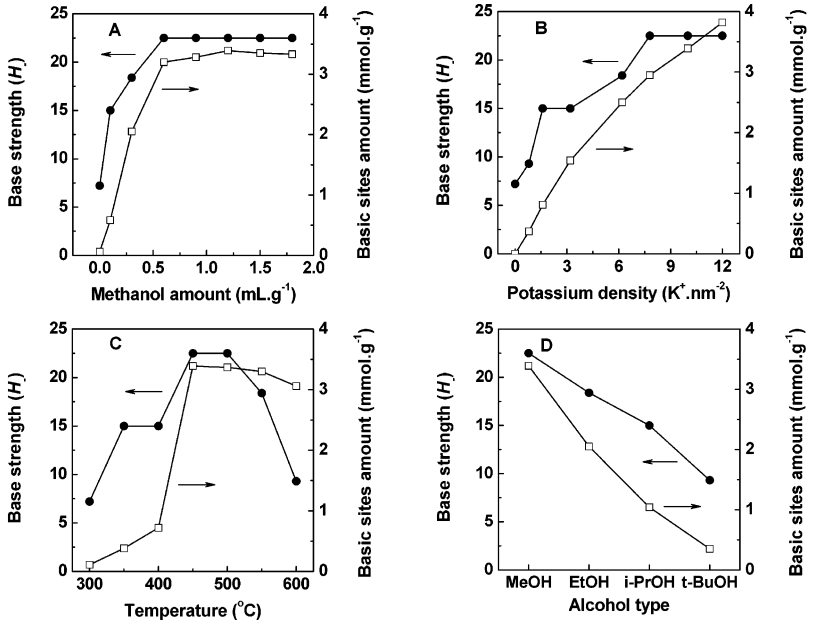

Figure 6. Effects of (A) methanol amount, (B) KNO_3 loading, (C) treatment temperature, and (D) reducing agent type on basic properties of KNO_3/SiO_2 samples. General conditions: methanol amount was 1.2 mL g^{-1}, potassium density was 10 K^+ nm^{-2}, temperature was 450 °C, and alcohol was methanol.

when the temperature exceeded 500 °C, the strength of the resulting basic sites dramatically declined while the amount slightly decreased; perhaps some strong basic species were converted to weak ones due to the reaction of potassium species with SiO_2 at high temperatures.[36] Figure 4B shows the IR spectra of $10KNO_3/SiO_2$ treated with methanol at different temperatures. After treatment at 300 °C, no obvious decline of nitrate bands was observed (curve b, Figure 4B), which coincided with the negligible amount of basic sites with a low base strength formed on the sample. The treatment at 400 °C led to a slight decrease of nitrate bands (curve c, Figure 4B), indicating the conversion of a small amount of KNO_3. As the temperature exceeded 450 °C, the bands of nitrate greatly declined, mirroring the complete conversion of KNO_3 and consistent with the results of the amount of basic sites.

Figure 6D depicts the impact of reducing the agent type on KNO_3 conversion, in which methanol, ethanol, 2-propanol, and *t*-butanol were employed. The IR spectra of KNO_3/SiO_2 treated with different alcohols are given in Figure 4C. The excellent performance of methanol in KNO_3 conversion can be associated with its strong reducibility since the alcohol molecule with a larger size tends to possess a lower reducibility.[37] The larger the alcohol is, the more the nitrate bands remain and the less the silanol groups consume. For the $10KNO_3/SiO_2$ sample, the optimum temperature and methanol dosage for KNO_3 conversion were 450 °C and 1.2 mL g^{-1}, respectively.

The conversion of KNO_3 on Al_2O_3, ZrO_2, and TiO_2 by the redox approach was also investigated. As seen in Figure 2A,B, methanol treatment at 450 °C made the diffraction lines of KNO_3 disappear from KNO_3/Al_2O_3 and KNO_3/ZrO_2 (Figure 2, curves d), indicating the full conversion of the guest. The basic sites generated on these two samples possess a high strength of $H_- = 27.0$ (Table 2). Only diffraction lines of TiO_2 remained on the patterns of KNO_3/TiO_2 treated with methanol at 450 °C (curve d, Figure 2C), which implies that the supported KNO_3 was converted and that no new compound such as $K_2Ti_8O_{17}$ was formed. Moreover, a strong strength of $H_- = 22.5$ emerged on KNO_3/TiO_2 (Table 2). Thus, a strong basicity was generated on KNO_3/TiO_2 for the first time.

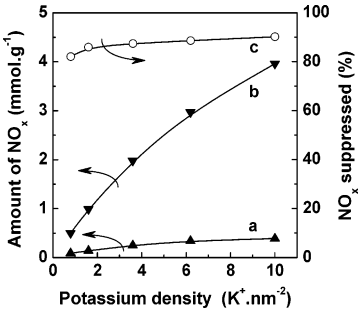

Figure 7. Suppression of NO_x from KNO_3 decomposition on SiO_2 by use of methanol. (a) Measured amount, (b) calculated amount, and (c) NO_x suppressed.

2-Propanol was employed to probe the surface acidity−basicity of the samples since it undergoes dehydrogenation to form acetone over basic sites, whereas acidic sites favor the dehydration of 2-propanol to propene. As shown in Table 2, 2-propanol was mainly converted to propene, and only a tiny amount of acetone was produced over Al_2O_3, ZrO_2, TiO_2, and SiO_2 themselves due to their acidity. After modification with KNO_3 and treatment with methanol, the formation rate of propene declined significantly; meanwhile, a significant amount of acetone formed due to the generation of basic active sites on these composites.

Thermal decomposition of KNO_3 loaded on porous supports unavoidably produced NO_x, which is a pollutant.[14] For instance, 3.96 mmol g^{-1} NO_x was released from $10KNO_3/SiO_2$ in thermal decomposition (Figure 7). In contrast, only 0.39 mmol g^{-1} NO_x was detected when the sample was treated with methanol. This means that more than 90% of NO_x was suppressed by the redox approach. Likewise, the redox approach can greatly suppress the NO_x from KNO_3 conversion on Al_2O_3, ZrO_2, and TiO_2 (Table 2). Actually, N_2 is proposed to be produced instead of NO_x during KNO_3 conversion by use of the redox approach, which will be discussed later.

For comparison, KNO_3 itself is treated with methanol under the same conditions, but it cannot convert at all. This indicates that the interaction between KNO_3 and support is important for the redox conversion of KNO_3. Figure 8 presents the TG curve

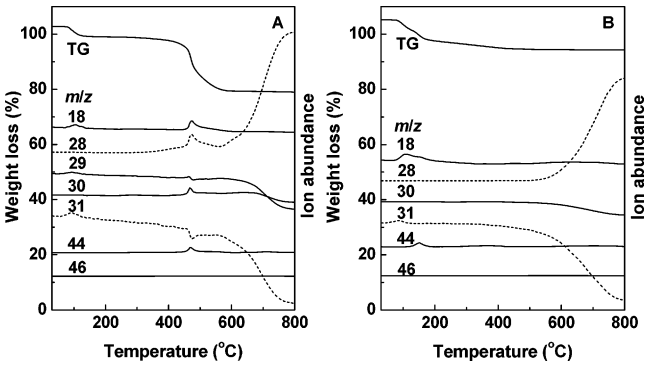

Figure 8. (A) TG-MS analysis data of KNO_3/SiO_2 treated with methanol. (B) Blank TG-MS test of KNO_3/SiO_2 treated with methanol; the analysis conditions were similar to those in panel A except that the sample was treated with methanol (1.2 mL g^{-1}) at 450 °C to convert KNO_3 before analysis.

and MS analysis of two KNO_3/SiO_2 samples under the same conditions except that sample B was pretreated with methanol at 450 °C prior to TG-MS analysis. That is to say, KNO_3 in sample B was converted before analysis. Both the redox reaction of supported KNO_3 with methanol and the decomposition of methanol itself occurred during the TG-MS analysis of sample A, whereas only the latter reaction occurred on sample B. Consequently, comparing the TG-MS spectra of samples A and B can distinguish the products derived from the redox reaction. The reaction of supported KNO_3 with methanol mainly occurred at around 470 °C and produced H_2O ($m/z = 18$), N_2 or CO ($m/z = 28$), NO ($m/z = 30$), and N_2O or CO_2 ($m/z = 44$), accompanied by the consumption of methanol ($m/z = 31$). In addition, the formation of two other possible products from methanol oxidization (i.e., formic acid and formaldehyde) also was taken into consideration. As shown in Figure 8A, the mass signal (m/z) of 46 is absent; thus, the yield of formic acid from the redox reaction was excluded. It is known that the mass signals (m/z) of 29 and 30 should have a similar alteration tendency if formaldehyde was produced. However, the changing tendency of $m/z = 29$ is more similar to $m/z = 31$ than 30 (Figure 8A), which indicates that the signal of $m/z = 29$ mainly should be derived from methanol rather than formaldehyde. Therefore, the amount of formaldehyde originating from the redox reaction is very scarce, if any. On the basis of the variation of the MS signal of methanol ($m/z = 31$) and the TG curve in Figure 8A, it is clear that the process can be divided into three stages. In the first stage, methanol desorbs from the composite at around 150 °C. In the second stage, the redox reaction of supported KNO_3 with methanol takes place near 470 °C, and in the third stage, methanol decomposes at above 560 °C.

Discussion

Among the oxide supports employed in the present study, SiO_2 has the largest surface area (411 m^2 g^{-1}), and KNO_3 should be easy to disperse on it. However, the dispersion capacity of KNO_3 on SiO_2 is the lowest. Actually, TiO_2 can disperse a large amount of KNO_3 despite its small surface area (52 m^2 g^{-1}). These facts suggest that the dispersion of KNO_3 is not correlated with the surface areas of different substrates. Likewise, no correlation between the pore volume of support and the dispersion of KNO_3 can be proposed.

The vacant sites on the surface of the support play essential roles in the dispersion and subsequent decomposition of KNO_3.[13] The surface of Al_2O_3 comprises the (110) and (100) planes,[38] and the (110) plane is preferentially exposed so that Al_2O_3 can be considered as consisting of particles formed by one-dimensional stacking of C- and D-layers with an equal exposure possibility.[39] There are vacant sites with a density of 18.80 nm^{-2} in the C-layer and 20.57 nm^{-2} in the D-layer of Al_2O_3, and the ratio of the usable octahedral sites to the tetrahedral sites is 1:3 and 1:4 in the C- and D-layer, repectively.[40] However, the K^+ cation with a radius of 0.13 nm only can insert in the octahedral vacant sites in the surface lattice of Al_2O_3;[41] therefore, the dispersion capacity of KNO_3 is estimated to be about 4.4 K^+ nm^{-2} theoretically (Table 1). Similarly, the (111) and (001) planes are preferentially exposed on the surface of ZrO_2 and TiO_2 (anatase), respectively.[42,43] There are two vacant sites in each unit mesh (ca. 0.230 nm^2) for ZrO_2[44] and one vacant site in each unit mesh (ca. 0.142 nm^2) for TiO_2,[40] corresponding to a vacant site density of about 8.6 and 7.0 nm^{-2}, respectively (Table 1). Different from Al_2O_3, ZrO_2, and TiO_2, there is no vacant site on the surface of SiO_2;[40] hence, KNO_3 cannot be dispersed on SiO_2 theoretically. As compared in Table 1, the dispersion capacity calculated from vacant sites of supports is consistent with the value measured from XRD quantitative analysis. As a result, the dispersion of guest KNO_3 on supports is proposed to proceed via the insertion of K^+ to surface vacant sites.[13,14] Further, such an insertion dispersion model leads to a strong guest−host interaction,[42] which is crucial for the subsequent thermal decomposition of KNO_3 to generate basicity on the supports.

Since octahedral vacant sites exist on the surface of both Al_2O_3 and ZrO_2, the K^+ of KNO_3 begins to insert in the octahedral vacant sites of supports during sample preparation, leading to a strong guest−host interaction. Consequently, KNO_3 tends to disperse dissociatively,[21] and the bond between K^+ and NO_3^- is weakened. In the process of thermal activation, these species begin to decompose and create strongly basic sites on the surface of Al_2O_3 and ZrO_2. Thus, the base strength of $H\_ = 27.0$ can be measured on KNO_3/Al_2O_3 and KNO_3/ZrO_2 after thermal activation at 600 °C. There are also octahedral vacant sites on the surface of TiO_2 provided for the insertion of K^+; thus, KNO_3 should be easy to decompose and generate a strong basicity. However, a base strength ($H\_$) of only 9.3 was measured on KNO_3/TiO_2 after activation at 600 °C, although the KNO_3 is converted, because $K_2Ti_8O_{17}$ with a weak basicity causes a low base strength of KNO_3/TiO_2. Since no vacant site exists on the surface of SiO_2, KNO_3 is difficult to decompose, and only the transformation of the crystalline phase takes place during thermal activation, corresponding to the weak basicity of KNO_3/SiO_2 ($H\_ = 9.3$).

The electronegativity of cations in the oxide is another factor affecting the decomposition of supported KNO_3 because it relates to the metal−oxygen (or silicon−oxygen) interaction in the oxide. As the electronegativity declines, the metal−oxygen (or silicon−oxygen) bond becomes weak; hence, the coordination ability of the lattice oxygen increases,[45] leading to a strong KNO_3−support interaction that is beneficial to the decomposition of KNO_3.[15] According to the investigation of Tanaka and Ozaki,[46] the electronegativity of some cations (χ_i) in oxides was calculated (Table 1), which increases in the following order $Al_2O_3 < ZrO_2 < TiO_2 < SiO_2$. As a result, KNO_3 is easier to decompose on Al_2O_3 or ZrO_2 after thermal activation at 600 °C than on SiO_2 or TiO_2.

KNO_3 is an oxidizing agent so that a redox approach was employed to convert the KNO_3 supported to generate basicity. For the sample of KNO_3/SiO_2, thermal activation at 600 °C only led to the change of the KNO_3 crystalline phase rather than KNO_3 decomposition. However, the guest KNO_3 can be

converted at 450 °C via a redox approach, and the strong basicity with a strength of $H_- = 22.5$ was generated. For the traditional thermal activation to convert a supported neutral salt such as KNO_3, the support has to possess some specific features. On one hand, the host should have many surface vacant sites to anchor the guest, which is important for the decomposition of KNO_3, similar to what occurs on Al_2O_3.[13,29] On the other hand, the cations in the support need to have an appropriate electronegativity to promote the interaction of the guest with the lattice of the host.[15] Only on the basis of the previously two specific features, the neutral salt can be thermally decomposed over the host to form basic sites. Unfortunately, only a few materials such as Al_2O_3 and ZrO_2 can meet these strict demands, and solid strong bases thus were successfully prepared from KNO_3 supported on Al_2O_3 and ZrO_2.[13,14] For the other materials that cannot provide such a microenvironment to anchor the guest, both dispersion and decomposition of the guest on them are difficult. Therefore, a higher temperature is required to decompose the supported neutral salt. However, the newly formed potassium species can easily react with silicon in the support at high temperatures,[36] not only forming a compound with a low base strength but also destroying the original structure of the host when zeolite or mesoporous silica is applied as the support.[23,28,30] This is the reason as to why it is impossible to generate strong basic sites on silica or titania. Taking account of the oxidizability of KNO_3, we used a reducing agent to induce the conversion of the neutral salt, provided that the guest can spread on the host since the redox reaction of KNO_3 with some reducing agents is much easier than its thermal decomposition. Actually, the present redox method shows a synergy that combines host−guest interactions and chemical reactions to convert the guest. Hence, a strong basicity successfully was generated on SiO_2 and TiO_2.

By means of the redox method, strongly basic sites with a strength H_- of 22.5 also were generated on KNO_3/TiO_2. Owing to the inherent characteristics of TiO_2, the host−guest interaction is insufficient to convert supported KNO_3 at 450 °C even if the guest has been well-dispersed. However, elevating the temperature to 600 °C will result in the reaction of KNO_3 with TiO_2 to yield a weakly basic compound $K_2Ti_8O_{17}$. The redox method produces strong basic species on titania at 450 °C and avoids the formation of $K_2Ti_8O_{17}$, and this method may open a new door for the preparation of basic materials derived from TiO_2. Although the redox method does not depend on the dispersion or anchoring of KNO_3 on supports, the good dispersion and anchoring of KNO_3 are beneficial to form superbasic materials. As a result, KNO_3-modified Al_2O_3 and ZrO_2 possess a strong basicity with strength H_- of 27.0. According to the definition of Tanabe and Noyori,[47] these materials can be regarded as solid superbases. It is energy-saving since the process is conducted at 450 °C, whereas 600 °C is required for the thermal activation of KNO_3/Al_2O_3[13] and KNO_3/ZrO_2[14] and even higher (700−900 °C) for superbases derived from CaO and SrO.[48]

As shown in Figure 1B, the employed supports possess relatively wide pore size distributions, and KNO_3 located in te pores of different sizes may have a different accessibility for the reducing agent molecule. Apparently, some of the pores with smaller sizes, especially micropores (Table 1), are not accessible for surface reactions. In the present study, the redox reaction was conducted at 450 °C, while the melting point of KNO_3 is 334 °C. Therefore, mass transfer within pores of different sizes was proposed to take place, which may play an important role in the complete conversion of supported KNO_3.

SCHEME 1: General Processes for Conversion of KNO_3 on Different Oxide Supports by Thermal Activation and Redox Approach

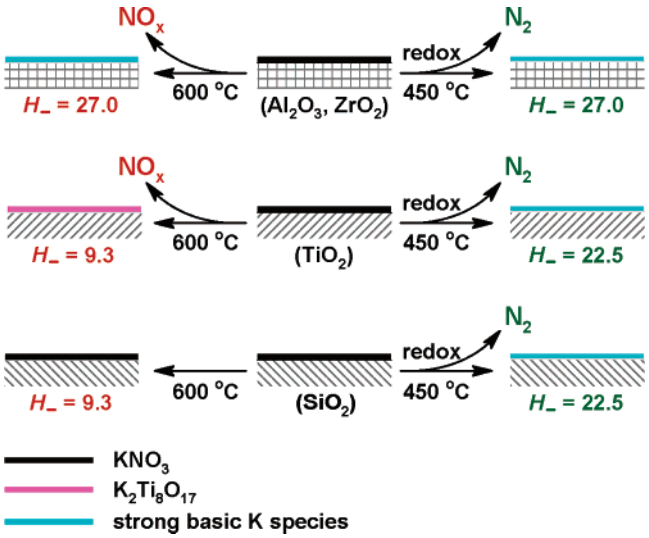

Another advantage of the redox method to convert supported KNO_3 was to suppress the release of NO_x, as the main product is N_2 that is environmentally benign. Scheme 1 summarizes general processes for the conversion of KNO_3 on Al_2O_3, ZrO_2, TiO_2, and SiO_2 by the thermal activation and redox methods. By use of the redox method, strongly basic sites with strength (H_-) of 22.5−27.0 were created on the four oxides at 450 °C, accompanied by the suppression of NO_x release. Moreover, this provides a clue as to how to utilize chemical reactions to assist or promote host−guest interactions in the design and synthesis of new functional materials.

Conclusion

(1) The factors that hinder the formation of strong basicity on silica and titania through neutral salt KNO_3 modification are disclosed. Such factors include the surface vacant sites and the electronegativity of cations in oxide supports, which govern the dispersion and decomposition of the base precursor. (2) A lack of proper microenvironment in silica and titania to anchor the base precursor such as KNO_3 disturbs the decomposition of the guest; therefore, a higher temperature is required. However, the newly formed basic species will react with the support at the high temperature to form a compound with a low base strength. (3) The redox method induces the reaction of supported KNO_3 with the reducing agent, so that KNO_3 can be converted to strong basic sites at a relatively low temperature of 450 °C. A strong basicity with a strength (H_-) of 22.5 was generated on silica and titania for the first time, while superbasicity ($H_- = 27.0$) was formed on alumina and zirconia. (4) The redox method can significantly suppress the release of NO_x during the decomposition of KNO_3 loaded on porous supports.

Acknowledgment. Financial support from NHTRDP973 (2007CB613301), NSF of China (20773601 and 20673053), 863 Projects of the Chinese Science Committee, and the Analysis Center of Nanjing University is gratefully acknowledged.

References and Notes

(1) Asefa, T.; MacLachan, M. J.; Coombs, N.; Ozin, G. A. *Nature (London, U.K.)* **1999**, *402*, 867.

(2) Liu, X. Y.; Tian, B. Z.; Yu, C. Z.; Gao, F.; Xie, S. H.; Tu, B.; Che, R. C.; Peng, L. M.; Zhao, D. Y. *Angew. Chem., Int. Ed.* **2002**, *41*, 3876.

(3) Kim, S. S.; Zhang, W. Z.; Pinnavaia, T. J. *Science (Washington, DC, U.S.)* **1998**, *282*, 1302.
(4) Mercier, L.; Pinnavaia, T. J. *Adv. Mater.* **1997**, *9*, 500.
(5) Wang, Y. J.; Caruso, F. *Adv. Mater.* **2006**, *18*, 795.
(6) Jin, H. Y.; Liu, Z.; Ohsuna, T.; Terasaki, O.; Inoue, Y.; Sakamoto, K.; Nakanishi, T.; Ariga, K.; Che, S. N. *Adv. Mater.* **2006**, *18*, 593.
(7) Jung, J. H.; Ono, Y.; Hanabusa, K.; Shinkai, S. *J. Am. Chem. Soc.* **2000**, *122*, 5008.
(8) Asefa, T.; Kruk, M.; MacLachlan, M. J.; Coombs, N.; Grondey, H.; Jaroniec, M.; Ozin, G. A. *J. Am. Chem. Soc.* **2001**, *123*, 8520.
(9) Soler-Illia, G. J. A. A.; Sanchez, C.; Lebeau, B.; Patarin, J. *Chem. Rev.* **2002**, *102*, 4093.
(10) Suzukamo, G.; Fukao, M.; Minobe, M. *Chem. Lett.* **1980**, 585.
(11) Baba, T.; Handa, H.; Ono, Y. *J. Chem. Soc., Faraday Trans.* **1994**, *90*, 187.
(12) Sels, B.; De Vos, D. E.; Jacobs, P. A. *Catal. Rev.* **2001**, *43*, 443.
(13) Zhu, J. H.; Wang, Y.; Chun, Y.; Wang, X. S. *J. Chem. Soc., Faraday Trans.* **1998**, *94*, 1163.
(14) Wang, Y.; Huang, W. Y.; Chun, Y.; Xia, J. R.; Zhu, J. H. *Chem. Mater.* **2001**, *13*, 670.
(15) Sun, L. B.; Wu, Z. Y.; Kou, J. H.; Chun, Y.; Wang, Y.; Zhu, J. H.; Zou, Z. G. *Chin. J. Catal.* **2006**, *27*, 725.
(16) Zacheis, G. A.; Gray, K. A.; Kamat, P. V. *J. Phys. Chem. B* **2001**, *105*, 4715.
(17) Miller, J. T.; Kropf, A. J.; Zha, Y.; Regalbuto, J. R.; Delannoy, L.; Louis, C.; Bus, E.; van Bokhoven, J. A. *J. Catal.* **2006**, *240*, 222.
(18) Hattori, H. *Chem. Rev.* **1995**, *95*, 537.
(19) Ono, Y. *J. Catal.* **2003**, *216*, 406.
(20) Davis, R. J. *J. Catal.* **2003**, *216*, 396.
(21) Yamaguchi, T.; Zhu, J. H.; Wang, Y.; Komatsu, M.; Ookawa, M. *Chem. Lett.* **1997**, 989.
(22) Wang, Y.; Huang, W. Y.; Wu, Z.; Chun, Y.; Zhu, J. H. *Mater. Lett.* **2000**, *46*, 198.
(23) Wu, Z. Y.; Jiang, Q.; Wang, Y. M.; Wang, H. J.; Sun, L. B.; Shi, L. Y.; Xu, J. H.; Wang, Y.; Chun, Y.; Zhu, J. H. *Chem. Mater.* **2006**, *18*, 4600.
(24) Zhu, J. H.; Chun, Y.; Wang, Y.; Xu, Q. H. *Mater. Lett.* **1997**, *33*, 207.
(25) Handa, H.; Baba, T.; Sugisawa, H.; Ono, Y. *J. Mol. Catal. A: Chem.* **1998**, *134*, 171.
(26) Baba, T.; Kato, A.; Takahashi, H.; Toriyama, F.; Handa, H.; Ono, Y.; Sugisawa, H. *J. Catal.* **1998**, *176*, 488.
(27) Kawanami, Y.; Yuasa, H.; Toriyama, F.; Yoshida, S.; Baba, T. *Catal. Commun.* **2003**, *4*, 455.
(28) Sun, L. B.; Chun, Y.; Gu, F. N.; Yue, M. B.; Yu, Q.; Wang, Y.; Zhu, J. H. *Mater. Lett.* **2007**, *61*, 2130.
(29) Wang, Y.; Zhu, J. H.; Huang, W. Y. *Phys. Chem. Chem. Phys.* **2001**, *3*, 2537.
(30) Shen, B.; Chun, Y.; Zhu, J. H.; Wang, Y.; Wu, Z.; Xia, J. R.; Xu, Q. H. *Phys. Chem. Commun.* **1999**, *2*, 9.
(31) Barton, T. J.; Bull, L. M.; Klemperer, W. G.; Loy, D. A.; McEnaney, B.; Misono, M.; Monson, P. A.; Pez, G.; Scherer, G. W.; Vartuli, J. C.; Yaghi, O. M. *Chem. Mater.* **1999**, *11*, 2633.
(32) Nakamoto, K. *Infrared Spectra of Inorganic and Coordination Compounds*; John Wiley: New York, 1970; p 98.
(33) White, R. G. *Handbook of Industrial Infrared Analysis*; Plenum Press: New York, 1964; p 214.
(34) Tian, B.; Liu, X.; Yu, C.; Gao, F.; Luo, Q.; Xie, S.; Tu, B.; Zhao, D. *Chem. Commun. (Cambridge, U.K.)* **2002**, 1186.
(35) Wang, Y. M.; Wu, Z. Y.; Zhu, J. H. *J. Solid State Chem.* **2004**, *177*, 3815.
(36) Zhu, J. H.; Chun, Y.; Qin, Y.; Xu, Q. H. *Microporous Mesoporous Mater.* **1998**, *24*, 19.
(37) Tran, D. N.; Aardahl, C. L.; Rappe, K. L.; Park, P. W.; Boyer, C. L. *Appl. Catal., B* **2004**, *48*, 155.
(38) Beaufils, J. P.; Bardaux, Y. *J. Chem. Phys.* **1981**, *78*, 347.
(39) Chen, Y.; Zhang, L. F. *Catal. Lett.* **1992**, *12*, 51.
(40) Dong, L. The Interaction of Ionic Compounds with Oxide Supports. Ph.D. Thesis, Nanjing University, 1995.
(41) West, A. R. *Solid State Chemistry and Its Applications*; John Wiley and Sons Inc.: New York, 1984; p 271.
(42) Liu, Z.; Dong, L.; Ji, W. J.; Chen, Y. *J. Chem. Soc., Faraday Trans.* **1998**, *94*, 1137.
(43) Primet, M.; Pichat, P.; Mathieu, M. V. *J. Phys. Chem.* **1971**, *75*, 1216.
(44) Liu, Z.; Ji, W. J.; Dong, L.; Chen, Y. *J. Solid State Chem.* **1998**, *138*, 41.
(45) Kumar, M.; Aberuagba, F.; Gupta, J. K.; Rawat, K. S.; Sharma, L. D.; Dhar, G. M. *J. Mol. Catal. A: Chem.* **2004**, *213*, 217.
(46) Tanaka, K.-I.; Ozaki, A. *J. Catal.* **1967**, *8*, 1.
(47) Tanabe, K.; Noyari, R. *Chokyo-san, Chokyo-enki*; Kodansha: Tokyo, 1980; p 114.
(48) Lizuka, T.; Endo, Y.; Hattori, H.; Tanabe, K. *Chem. Lett.* **1976**, 803.